PHYSICAL REVIEW A VOLUME 43, NUMBER 2 15 JANUARY 1991

# Thermodynamics of Lorenz-type maps

P. Szépfalusy
*Institue for Solid State Physics, Eötvös University, P.O.Box 327, H-1445, Budapest, Hungary*

T. Tél* and G. Vattay†
*Institut für Festkorperforschung, Research Center Jülich, Postfach 1913, D-5170 Jülich, Federal Republic of Germany*
(Received 6 June 1990)

The thermodynamic properties of maps derived from strongly dissipative Lorenz-type flows are studied by means of generalized Frobenius-Perron operators. Three different types of phase transitions are found: (I) second-order transitions occurring at zero temperatures caused by short-range interactions in an associated spin chain characterizing hyperbolic maps, (II) first-order transitions caused by long-range interactions at finite temperatures induced by anomalous but exponential scaling in nonhyperbolic cases, and (III) transitions of extreme orders induced by nonexponential scaling in certain nonhyperbolic maps. Type-III transitions might also appear in the spectra of generalized entropies at nonzero temperatures. A novel feature of Lorenz-type maps is the existence of type-II–type-III and type-III–type-III double transitions.

## I. INTRODUCTION

In recent years, the application of the thermodynamic formalism[1–6] in analyzing strange sets has been widely accepted. Besides giving an illuminating analogy with the statistical mechanics of spin chains, the method provides us with an increased accuracy and, more importantly, with a deeper understanding of nonanalytic behavior in the scaling properties, which can be interpreted as phase transitions.[7–22]

In the field of dynamical systems this approach has been applied to a variety of low-dimensional maps. In one-dimensional cases and complex analytic maps the use of the generalized Frobenius-Perron (GFP) equation[23–31,5] turned out to be of special importance. It provides a mathematically convenient framework and numerically very fast iterative solutions.

The aim of this paper is to study maps associated with Lorenz-type systems in the case of strong dissipation. By Lorenz type we mean a three-variable time continuous flow possessing a hyperbolic fixed point (which can always be chosen to be the origin) with a two-dimensional stable and a one-dimensional unstable manifold. Such systems seem to be quite common: examples include, besides the Lorenz model,[32] the Rikitake dynamo[33] and a model by Rössler.[34] It is worth emphasizing that the symmetry of the original Lorenz system need not be preserved.

It has been shown[35–39] that the Poincaré map generated by the flow on a surface intersecting the attractor has nonanalytic features. Since trajectories approaching the origin on different sides of the stable manifold are pushed far away from each other, the map is discontinuous. Furthermore, as trajectories coming close to the origin spend a long time around it, their local properties will be governed by the eigenvalues of the linearized flow there ($\lambda_1 > 0$, $\lambda_2, \lambda_3 < 0$). This is reflected in the local form of the map by the appearance of power-law behavior with not necessarily integer exponents. In the case of extremely strong dissipation (vanishing Jacobian) the attractor consists of two separate pieces of line. The discrete time dynamics of a variable $x_n$ on it is governed by a map of type[36,37]

$$x_{n+1} = g(x_n, \mathrm{sgn}(x_{n-1})) \tag{1}$$

where $\mathrm{sgn}(x)$ denotes the sign of $x$, and $g$ is a bivariate function having a jump in $x$ at $x = 0$. The dependence on the sign is a natural consequence of the fact that the attractor has two pieces and the fate of a point depends not only on its position but also on which branch it came from. Note that Eq.(1) is a map with a one-step memory, but since only the sign plays a role, the memory is, in fact, a discrete variable. We find that all the general properties of map (1), including the existence of phase transitions, hold also for Lorenz-type maps where the memory is not present (see Sec. VII).

We shall be interested in two types of spectra. One is the free energy $F(\beta)$ connected with the length-scale distribution of map (1). This can be defined as follows. We associate to each element $x_i$ of a trajectory $\{x_j, j = 1, 2, \ldots\}$ a symbol $\epsilon_i = 1$ $(-1)$ if $x_i$ is positive (negative). The initial condition to the dynamics requires the knowledge of two values $(x_1, x_2)$ since the map possesses a one-step memory. Due to the special form of (1), however, only the sign of the first coordinate $\mathrm{sgn}(x_1) \equiv \epsilon_1$ is relevant. Then we find trajectories of length $n$ with a given symbol sequence $\epsilon_1, \ldots, \epsilon_n$. We take the interval $I(\epsilon_1, \ldots, \epsilon_n)$ from which these trajectories start (called cylinders) and measure its length $l(\epsilon_1, \ldots, \epsilon_n)$. The free energy[3] is defined as the growth rate of a sum containing all of these length scales raised to certain real power $\beta$:

$$\sum_{\{\epsilon_i\}} l(\epsilon_1, \ldots, \epsilon_n)^\beta \sim e^{-\beta F(\beta) n}. \tag{2}$$

 

The other type of spectrum we wish to study is connected with the existence of an invariant distribution on the cylinders. Let $P(\epsilon_1, ..., \epsilon_n)$ denote the measure of a cylinder with the given symbol sequence. Raising them to a power $q$ and summing over all symbol sequences the generalized Rényi entropies $K_q$ (Refs. 40–42) of the measure can be read off from the relation

$$\sum_{\{\epsilon_i\}} P(\epsilon_1, ..., \epsilon_n)^q \sim e^{(1-q)K_q n}. \tag{3}$$

If the map possesses a chaotic attractor, the most relevant distribution is its natural measure.[41]

We shall concentrate on complete topology cases when all binary symbol sequences are allowed to exist. Now, in contrast to single-humped maps, no general theorems are known which would ensure the existence of a chaotic attractor with a natural invariant distribution. Whether a natural measure exists should be checked numerically in particular cases. If the map turns out to possess a chaotic attractor, completeness is equivalent to fully developed chaos.[43]

In complete cases we find that maps of type (1) can be reduced to equivalent ones without memory. These maps have the peculiarity to possess zero or infinite slopes away from their point of discontinuity ($x = 0$) and have not yet been studied in detail. The free energy, and if a chaotic attractor exists the entropies too, will be shown to be eigenvalues of the GFP equation. Furthermore, we point out that the free energy generically exhibits a first-order phase transition, but the entropy spectrum does not. Due to the special features of the map a double phase transition might also occur. This must be connected with situations when one of the fixed points is either extremely unstable or is marginal, the latter corresponding to intermittency.[44]

The paper is organized as follows. In Sec. II the aforementioned equivalent map without memory is introduced. Then the properties of its GFP equation are discussed. The phase transition in the free energy is analyzed in Sec. IV. The possibility for a double phase transition is investigated in Sec. V. Next, in Sec. VI a piecewise linear case is considered where phase transitions of the type discussed earlier cannot occur. The thermodynamics will be shown to be the same as that of an Ising chain in which second-order transitions can be found at zero temperature. The paper is concluded in Sec. VII with a discussion.

## II. EQUIVALENT MAPS WITHOUT MEMORY

It is worth introducing new notations for the branches of map (1) (see Fig. 1)

$$\begin{aligned} g(x,+1) &= \phi_1(x), \quad x > 0 \\ g(x,-1) &= \phi_2(x), \quad x > 0 \\ g(x,+1) &= \phi_3(x), \quad x < 0 \\ g(x,-1) &= \phi_4(x), \quad x < 0. \end{aligned} \tag{4}$$

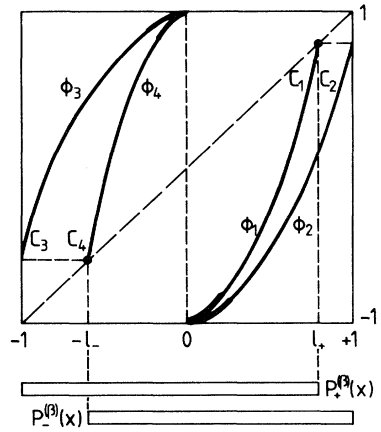


FIG. 1. A (complete) map of type (1) defined on the interval $[-1, 1]$. Points with positive preimages are mapped under $\phi_1, \phi_3$, those with negative preimages under $\phi_2, \phi_4$. The horizontal bars represent the supports of the functions $P_\pm^{(\beta)}(x)$. $c_1, \ldots, c_4$ denote the slopes at the end points of branches. The order $z$ extrema of the map are stressed by heavy lines.

One can easily check[36] that the Frobenius-Perron equation yielding the density of the natural measure for this map, provided the latter exists, has the appearance

$$P_+(x') = \frac{P_+(x_1)}{|\phi_1'(x_1)|} + \frac{P_-(x_2)}{|\phi_2'(x_2)|}, \tag{5}$$

$$P_-(x') = \frac{P_+(x_3)}{|\phi_3'(x_3)|} + \frac{P_-(x_4)}{|\phi_4'(x_4)|}, \tag{6}$$

where $P_{+(-)}(x)$ is the density around $x$ for points with positive (negative) preimages. The $x_i$'s denote the preimages of $x'$ so that $x' = \phi_i(x_i)$, $i = 1, ..., 4$.

In analogy with single valued maps, we define the GFP equation as

$$\lambda(\beta) P_+^{(\beta)}(x') = \frac{P_+^{(\beta)}(x_1)}{|\phi_1'(x_1)|^\beta} + \frac{P_-^{(\beta)}(x_2)}{|\phi_2'(x_2)|^\beta}, \tag{7}$$

$$\lambda(\beta) P_-^{(\beta)}(x') = \frac{P_+^{(\beta)}(x_3)}{|\phi_3'(x_3)|^\beta} + \frac{P_-^{(\beta)}(x_4)}{|\phi_4'(x_4)|^\beta}, \tag{8}$$

where $\lambda(\beta)$ is a real number, typically fixed by the criterion that a finite positive and smooth $P_\pm^{(\beta)}(x)$ is obtained when solving Eqs. (7) and (8) via an iteration procedure. Equations (7) and (8) can be considered as an eigenvalue problem of the generalized Frobenius-Perron operator where $\lambda(\beta)$ and $P_\pm^{(\beta)}(x)$ are eigenvalue and eigenfunction, respectively. This operator is well defined even if the map does not possess a chaotic attractor.[24,29] If it does, the special case $\beta = 1$ corresponds to (5) and (6) with eigenvalue $\lambda(\beta) = 1$.

For complete maps all symbol sequences are allowed to exist. The support of the map is mapped then two-to-one onto itself. This occurs, just like for single-humped maps, when the maximum is mapped onto a fixed point. In the present case the *second* image of $x = 1$ ($x = -1$)

has to be a fixed point $x = -l_-$ ($x = l_+$) lying on the $\phi_4$ ($\phi_1$) branch. Let the complete map be defined on the interval $[-1,1]$. The support of branches $\phi_1, \phi_2, \phi_3$, and $\phi_4$ is then $[0, l_+]$, $[0,1]$, $[-1,0]$, and $[-l_-, 0]$, respectively. They are projected in the following way:

$$\begin{aligned} \phi_1 &: [0, l_+] \to [-1, l_+], \\ \phi_2 &: [0, 1] \to [-1, l_+], \\ \phi_3 &: [-1, 0] \to [-l_-, 1], \\ \phi_4 &: [-l_-, 0] \to [-l_-, 1], \end{aligned} \tag{9}$$

where $l_+$ and $l_-$ can be arbitrary positive numbers not greater than 1 (see Fig. 1). Points with positive (negative) preimage then lie in $[-1, l_+]$ ($[-l_-, 1]$). As follows from (9), the inverses of both $\phi_1$ and $\phi_2$ ($\phi_3$ and $\phi_4$) are defined just on this interval. Consequently, although not all branches go from $-1$ to $+1$, all points with a given preimage sign have exactly two preimages, which ensures the completeness of topology. Notice that, due to the dependence on $\mathrm{sgn}(x_{n-1})$, the cylinders $I(\epsilon_1, \ldots, \epsilon_n)$ can overlap along the $x$ axis. Each $x$ value can belong to two different cylinders.

Next we show that in complete cases the problem of solving the GFP equation can be reduced to that of a single-valued map *without* memory, which means considerable simplification. We take a map obtained by the following linear transformation of branches (4) (Fig. 2):

$$f(x) = \begin{cases} +1 + \phi_1(x-1), & 1 < x < 1 + l_+ \\ -1 + \phi_3(x-1), & 0 < x < 1 \\ +1 + \phi_2(x+1), & -1 < x < 0 \\ -1 + \phi_4(x+1), & -1 - l_- < x < -1. \end{cases} \tag{10}$$

The transformation is invertible and preserves the distance between points whose preimages have the same sign. The Frobenius-Perron equation for any single-valued map $f$ has the form[45]

$$\varrho(x') = \sum_{x \in f^{-1}(x')} \frac{\varrho(x)}{|f'(x)|}, \tag{11}$$

where the summation is over the preimages of $x'$. By using (10) as $f$, one immediately sees that for $x' > 0$ and $x' < 0$ Eq. (11) is equivalent to Eqs. (5) and (6), respectively. The density $\varrho$ can, in fact, be expressed by the densities $P_+$ and $P_-$ as

$$\varrho(x) = \begin{cases} P_+(x-1), & x > 0 \\ P_-(x+1), & x < 0. \end{cases} \tag{12}$$

Thus we conclude that all topological and dynamical properties of maps (4), (9), and (10) are equivalent. In particular, due to the preservation of distances, the cylinder lenghts $l(\epsilon_1, \ldots, \epsilon_n)$ are the same. Consequently, the free energies of the two maps also coincide. Furthermore, the GFP equation for map (10)

$$\lambda(\beta)\varrho^{(\beta)}(x') = \sum_{x \in f^{-1}(x')} \frac{\varrho^{(\beta)}(x)}{|f'(x)|^\beta} \tag{13}$$

corresponds to Eqs. (7) and (8) with the same $\lambda(\beta)$ and

$$\varrho^{(\beta)}(x) = \begin{cases} P_+^{(\beta)}(x-1), & x > 0 \\ P_-^{(\beta)}(x+1), & x < 0. \end{cases} \tag{14}$$

It is worth mentioning that the GFP equation (13) is equivalent to that used by Feigenbaum when describing the theory of presentation functions.[5] For any single-humped complete map $f$ the presentation functions are just the two inverses of $f$.

Note that map (10) is defined on a larger interval than map (1). Consequently, a single initial point $x_1$ now completely defines a trajectory $\{x_1, x_2, \ldots\}$, the symbolic representation of which is given by $\epsilon_i \equiv \mathrm{sgn}(x_i)$. By reorganizing the map one also avoids the overlap of cylinders [the latter are now simply the preimages of the interval $I = (-1 - l_-, 1 + l_+)$]. This is a reason why it will be easier to use map (10), but the results we obtain are also valid for map (1) in its complete configuration.

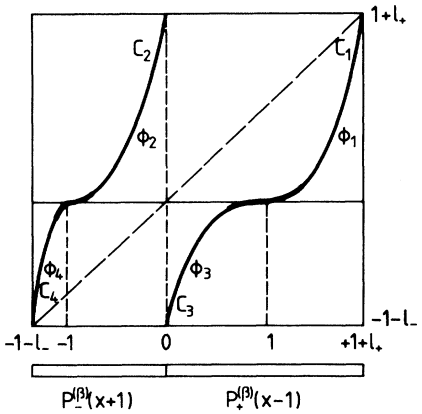


FIG. 2. Equivalent map $f(x)$ [Eq.(10)] in a complete case. The bars represent the supports of the functions $P_\pm^{(\beta)}(x)$ and illustrate how $\varrho^{(\beta)}(x)$ is built up from them. The meaning of heavy lines is the same as in Fig. 1.

## III. GENERALIZED FROBENIUS-PERRON OPERATOR

Based on the observation of Sec. II, the generalized Frobenius-Perron operator (GFPO) $L_\beta$ for complete Lorenz-type maps (10) can be written as

$$L_\beta \psi^{(\beta)}(x') = \sum_{x \in f^{-1}(x')} \frac{\psi^{(\beta)}(x)}{|f'(x)|^\beta}, \tag{15}$$

where $\psi^{(\beta)}(x)$ is the function on which the operator acts, and $f$ is defined in (10). Eigenvalues of (15), which can be constructed by an iterative way, have special importance as they have been shown to be connected with the multifractal, or more generally, thermodynamic proper-

ties of the map. In practice, the iteration scheme is the following. We iterate a starting function $\psi_0^{(\beta)}$ according to

$$\psi_{n+1}^{(\beta)} = R(\beta) L_\beta \psi_n^{(\beta)}, \tag{16}$$

where $R(\beta)$ is a positive real number which ensures the convergence of the series $\psi_n^{(\beta)}(x)$ towards a finite limiting function $\psi^{(\beta)}(x)$. In particular, if the starting function $\psi_0^{(\beta)}(x)$ is smooth, it was shown[24,29,31] that for single-valued maps

$$\ln R(\beta) = \beta F(\beta), \tag{17}$$

where $F(\beta)$ is the free energy defined by (2). $R^{-1}(\beta)$ is then just the largest eigenvalue $\lambda^*(\beta)$ of the operator $L_\beta$ in the function space generated by smooth initial functions.

If instead of a smooth $\psi_0^{(\beta)}$ a singular one is taken with the same singularities as the $\beta$'s power of the distribution $\varrho(x)$, another coefficient $R_1(\beta)$ will ensure the convergence of iteration (16). $R_1^{-1}(\beta)$ is then the largest eigenvalue $\lambda_1(\beta) \equiv \exp[-\beta F_1(\beta)]$ of $L_\beta$ for functions having the same singularities as $\varrho^\beta(x)$ . This eigenvalue was proven[27,29] to be connected with the generalized entropies of the map as

$$\ln \lambda_1(\beta) \equiv -\beta F_1(\beta) = (1-q) K_q \mid_{q=\beta}, \tag{18}$$

provided there is a chaotic attractor in the map.

Let us briefly mention what can happen if no chaotic attractor exists. One possibility is that the density $\varrho(x)$ is not normalizable, reflecting the presence of a marginally stable periodic orbit occurring in strong intermittent situations (see Sec. V). Another case, which we shall not study here, is connected with the existence of stable periodic orbits, i.e., simple attractors. Nevertheless, a weak chaos might then be present in the form of chaotic transients. The free energy then contains information about a chaotic repeller[46] underlying the transients, and the fractal dimensions of the repeller follow from $F(\beta)$.[23,24] The entropy spectrum with respect to the natural measure on the repeller can also be deduced via relation[24]

$$(q-1) K_q = q F(q) - \kappa q, \tag{19}$$

where $\kappa \equiv F(1)$ is the escape rate characterizing the strenght of repulsion around the repeller.

## IV. FIRST-ORDER PHASE TRANSITIONS

We concentrate on the physically relevant case when all branches (4) have the same type of singularities around the origin: $\phi_i$ changes like $a_i \mid x \mid^z$ where $a_i$ are constants. The order $z$ of singularities was shown to be determined by the two largest eigenvalues of the underlying Lorenz-type flow at the origin ($z = \mid \lambda_2 \mid / \lambda_1 > 0$). We shall see that the most essential features of phase transitions in the free energy depend solely on $z$ and the slopes of the branches in two main fixed points. Therefore the particular forms of branches do not play an important role. As an illustrative example we shall use the following class of maps:

$$\begin{aligned} \phi_1 &= -1 + (1 + l_+) \mid x/l_+ \mid^z, \\ \phi_2 &= -1 + (1 + l_+) \mid x \mid^z, \\ \phi_3 &= +1 - (1 + l_-) \mid x \mid^z, \\ \phi_4 &= +1 - (1 + l_-) \mid x/l_- \mid^z. \end{aligned} \tag{20}$$

Consequently, map (10) has the form

$$f(x) = \begin{cases} +(1+l_+) \mid (x-1)/l_+ \mid^z, & 1 < x < 1 + l_+ \\ -(1+l_-) \mid 1 - x \mid^z, & 0 < x < 1 \\ +(1+l_+) \mid x + 1 \mid^z, & -1 < x < 0 \\ -(1+l_-) \mid (x+1)/l_- \mid^z, & -1 - l_- < x < -1 \end{cases} \tag{21}$$

where $l_+, l_- \leq 1$ are positive parameters.

Our numerical investigations of the GFPO show that a phase transition can, in general, be observed in $\beta F(\beta)$ for $z > 1$ at some $\beta_c < 0$ and for $z < 1$ at $\beta_c > 0$. For $z > (<) 1$ the free energy seems to be a constant for $\beta < (>) \beta_c$, i.e.,

$$\beta F(\beta) = \beta F_0, \tag{22}$$

in this range. Figure 3 shows the free energy of a particular case with $z = 2$. This picture was obtained after $n = 12$ iteration steps of the GFPO starting from a constant function. The convergence is very fast in $n$, therefore an accurancy of $10^{-5}$ has been obtained away from the critical point $\beta_c$. The same result is found if we evaluate the free energy via definition (2). Around the critical point the convergence is much slower and an accuracy of only a few percent can be reached at $\beta_c$.

The explanation of this behavior is based on a singularity analysis of the iteration procedure. Consider a general map of type (10). Let

$$\begin{aligned} c_1 &= \mid f'(1 + l_+) \mid, \\ c_2 &= \mid f'(+0) \mid, \\ c_3 &= \mid f'(-0) \mid, \\ c_4 &= \mid f'(-1 - l_-) \mid \end{aligned} \tag{23}$$

denote the slopes at the end points of the branches. For simplicity, we assume that the two fixed points at $x = 1 + l_+$ and $-1 - l_-$ are unstable ($c_1, c_4 > 1$). In the vicinity of $x = \pm 1$ map $f$ is supposed to behave like

$$\begin{aligned} f(x \to +1 + 0) &\approx a_1 \mid x - 1 \mid^z, \\ f(x \to -1 + 0) &\approx a_2 \mid x + 1 \mid^z, \\ f(x \to +1 - 0) &\approx a_3 \mid x - 1 \mid^z, \\ f(x \to -1 - 0) &\approx a_4 \mid x + 1 \mid^z, \end{aligned} \tag{24}$$

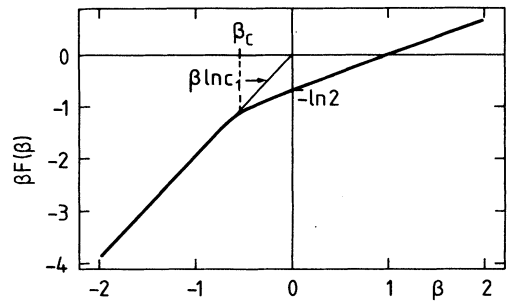


FIG. 3. Free energy of map (21) with $l_+ = 0.4$, $l_- = 0.8$, and $z = 2$ obtained numerically. The break around $\beta_c \approx -0.567$ is a sign of a phase transition. Notice the straight-line behavior for $\beta < \beta_c$.

where $a_1, a_2$ and $a_3, a_4$ are positive and negative constants, respectively. The function $\psi_n^{(\beta)}$ obtained from a smooth initial one under iteration (16) is smooth with the exception of four values $x = -0, +0, -1-l_-, +1+l_+$ where it can have singularities of power-law type. Therefore we write the local forms as

$$\begin{aligned}
&\psi_n^{(\beta)}(x \to 1+l_+) \approx A_1^{(n)}(x-1-l_+)^{-\sigma_1^{(n)}},\\
&\psi_n^{(\beta)}(x \to -0) \approx A_2^{(n)}(-x)^{-\sigma_2^{(n)}},\\
&\psi_n^{(\beta)}(x \to +0) \approx A_3^{(n)}(+x)^{-\sigma_3^{(n)}},\\
&\psi_n^{(\beta)}(x \to -1-l_-) \approx A_4^{(n)}(x+1+l_-)^{-\sigma_4^{(n)}}.
\end{aligned} \tag{25}$$

It is easy to find out how the singularities of the next approximant $\psi_{n+1}^{(\beta)}$ will look. Since the preimages of $x \approx 0$ are

$$f^{-1}(x \to +0) \approx \begin{cases} +1+\left|\frac{x}{a_1}\right|^{1/z} \\ -1+\left|\frac{x}{a_2}\right|^{1/z}, \end{cases}$$

$$f^{-1}(x \to -0) \approx \begin{cases} +1+\left|\frac{x}{a_3}\right|^{1/z} \\ -1+\left|\frac{x}{a_4}\right|^{1/z}, \end{cases} \tag{26}$$

we obtain

$$\psi_{n+1}^{(\beta)}(x)|_{x\to+0} \approx \frac{1}{\lambda(\beta)}\left(\frac{\psi_n^{(\beta)}(-1)}{(z{a_2}^{1/z})^\beta}+\frac{\psi_n^{(\beta)}(+1)}{(z{a_1}^{1/z})^\beta}\right)\mid x\mid^{-(1-1/z)\beta}, \tag{27}$$

and the same expression for $\psi_{n+1}^{(\beta)}(x)_{x\to-0}$, but with $\mid a_3 \mid$ and $\mid a_4 \mid$ instead of $a_1$ and $a_2$. Here we used the fact that $\psi_n^{(\beta)}(x)$ is smooth at $\pm 1$. The preimages of $x$ around $-(1+l_-)$ and $1+l_+$ are

$$\begin{aligned}
f^{-1}(x \to +1+l_+) &\approx +1+l_+ +(x-1-l_+)/c_1, \text{ and}\\
&\approx (x-1-l_+)/c_2,\\
f^{-1}(x' \to -1-l_-) &\approx -1-l_- +(x+1+l_-)/c_4, \text{ and}\\
&\approx (x+1+l_2)/c_3.
\end{aligned} \tag{28}$$

Thus one finds

$$\psi_{n+1}^{(\beta)}(x)|_{x\to+1+l_+} \approx A_{(1)}^{n+1}(x-1-l_+)^{-\sigma_1^{(n+1)}} \approx \frac{1}{\lambda(\beta)}\left[\frac{A_2^{(n)}}{c_2^\beta}\left(\frac{x-1-l_+}{c_2}\right)^{-\sigma_2^{(n)}}+\frac{A_1^{(n)}}{c_1^\beta}\left(\frac{x-1-l_+}{c_1}\right)^{-\sigma_1^{(n)}}\right], \tag{29}$$

$$\psi_{n+1}^{(\beta)}(x)|_{x\to-1-l_-} \approx A_{(4)}^{n+1}(x+1+l_-)^{-\sigma_4^{(n+1)}} \approx \frac{1}{\lambda(\beta)}\left[\frac{A_4^{(n)}}{c_4^\beta}\left(\frac{x+1+l_-}{c_4}\right)^{-\sigma_4^{(n)}}+\frac{A_3^{(n)}}{c_3^\beta}\left(\frac{x+1+l_-}{c_3}\right)^{-\sigma_3^{(n)}}\right]. \tag{30}$$

Equation (27) tells us that the new singularities around $x = 0$ are

$$\sigma_2^{(n+1)} = \sigma_3^{(n+1)} = \left(1-\frac{1}{z}\right)\beta \equiv \sigma(\beta), \tag{31}$$

independent of the previous ones. On the right-hand side of Eqs. (29) and (30) the maximal exponent will dominate, consequently

$$\sigma_1^{(n+1)} = \max(\sigma_1^{(n)}, \sigma_2^{(n)}), \tag{32}$$

$$\sigma_4^{(n+1)} = \max(\sigma_3^{(n)}, \sigma_4^{(n)}). \tag{33}$$

Let us now follow how singularities are built up when iterating a smooth initial function $\psi_0^{(\beta)}(x)$ ($\sigma_1^{(0)} = \cdots = \sigma_4^{(0)} = 0$). In the first step singularities of order $\sigma(\beta)$ appear at both sides of the origin and stay there forever. Singularities at the two corners are first not present, and in the next step

$$\sigma_1^{(2)} = \sigma_4^{(2)} = \max(0, \sigma(\beta)). \tag{34}$$

As long as $\sigma(\beta) > 0$, i.e., $\beta > 0$ ($\beta < 0$) for $z > 1$ ($z < 1$), these exponents coincide with $\sigma(\beta)$ and will not change under iteration. If, however, $\sigma(\beta) < 0$, the contribution from singularities around the origin is negligible, no singularities show up at the corners: $\sigma_1^{(2)} = \sigma_4^{(2)} = 0$, and this might remain so in subsequent steps. From relations (29)–(33) we find then a compatibility condition in the form

$$\lambda(\beta)A_{1(4)}^{(n+1)} = c_{1(4)}^{-\beta}A_{1(4)}^{(n)}. \tag{35}$$

Assuming the amplitudes $A_1^{(n)}$ and $A_4^{(n)}$ have a finite limit for $n \to \infty$, this equation tells us that

$$\lambda_0^{1(2)}(\beta) = c_{1(4)}^{-\beta} \tag{36}$$

are possible eigenvalues for $\sigma(\beta) < 0$ of the GFPO. The largest of them

$$\lambda_0(\beta) \equiv e^{-\beta F_0} = \max(c_1^{-\beta}, c_4^{-\beta}) \tag{37}$$

might in a region dominate the iteration which corresponds to a constant free energy, in harmony with the numerical finding exhibited in Fig. 3.

When starting with an initial function having order $\sigma(\beta)$ singularities at the origin and at the fixed points $[\sigma_1^{(0)} = \sigma_2^{(0)} = \sigma_3^{(0)} = \sigma_4^{(0)} = \sigma(\beta)]$, the complication found above never arises since the singularities remain unchanged under iteration [see (31)–(33)]. Inside this function space there should exist a largest eigenvalue $\lambda_1(\beta) \equiv \exp[-\beta F_1(\beta)]$ of the GFPO which is obtainable numerically.

Note that for $\sigma(\beta) > 0$ smooth initial functions also iterate into functions having order $\sigma(\beta)$ singularities at the origin and at the fixed points. The free energy is associated with the largest eigenvalue $\lambda^*(\beta) \equiv \exp[-\beta F(\beta)]$ when started with a smooth initial function. Consequently, for $\sigma(\beta) > 0$ the eigenvalues $\lambda^*$ and $\lambda_1$ always coincide and $F(\beta) = F_1(\beta)$ in this region. In the complementer region, however, $\lambda^*$ is obviously the maximum of (37) and $\lambda_1(\beta)$, thus we find

$$\begin{aligned}\beta F(\beta) &= \min(\beta \ln c_1, \beta \ln c_4, -\ln \lambda_1(\beta)) \\ &= \min(\beta F_0, \beta F_1(\beta)).\end{aligned} \tag{38}$$

When $\lambda_0(\beta)$ and $\lambda_1(\beta)$ become equal at a certain $\beta_c$, a break appears in the plot $\beta F(\beta)$ versus $\beta$, corresponding to a first-order phase transition in the free energy at $\beta_c$ (Fig. 4). Note that such a phase transition can only occur in the range $\beta < 0$ for $z > 1$ and $\beta > 0$ for $z < 1$, since the branch $\lambda_0(\beta)$ exists for $\sigma(\beta) < 0$ only. In hyperbolic cases ($z = 1$) this type of transition never takes place as $\lambda_0$ [Eq.(37)] does not exist.

The eigenvalue $\lambda_1(\beta) \equiv \exp[-\beta F_1(\beta)]$ can directly be obtained by iterating a function having order $\sigma(\beta)$ singularities at the origin and at the fixed points. Figure 5 shows $\beta F_1(\beta)$ versus $\beta$ for the same parameters as Fig. 3. This makes a highly accurate determination of the critical temperature possible since $\lambda_0(\beta)$ is known analytically and the intersection of the graph $\beta F_0$ and $\beta F_1(\beta)$ yields $\beta_c$. In our case $\beta_c = -0.567 \pm 0.001$. Thus the critical slowing down being present by iterating a smooth initial function can be avoided. When map $f$ possesses a chaotic attractor $\lambda_1(\beta)$ is connected with the generalized entropies as

$$(q-1)K_q = qF_1(q). \tag{39}$$

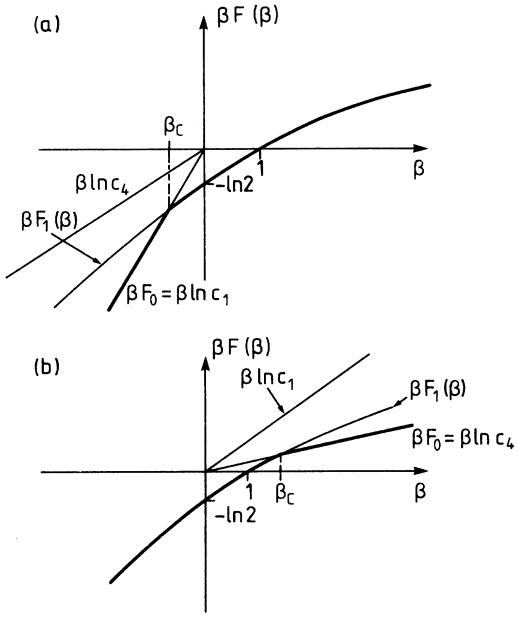


FIG. 4. Schematic diagram illustrating the mechanism of first-order phase transitions for (a) $z > 1$ and (b) $z < 1$. In both cases $c_1 > c_4$ was taken. The quantity $\beta F(\beta)$ (heavy line) is the absolute minimum of $\beta F_1(\beta)$ and $\beta F_0$; see (38).

This equation can be checked numerically by measuring the probabilities of the symbol sequences and using the direct formula (3). For the example of Fig. 5, for instance, we found numerically a chaotic attractor on the interval $(-1 - l_-, +1 + l_+)$ and our direct measurement of $K_q$ supports the validity of (39).

## V. DOUBLE PHASE TRANSITIONS

Although there are two independent parameters $c_1$ and $c_4$, a double phase transition caused by the intersection of both branches $\beta \ln c_1$ and $\beta \ln c_4$ with $\beta F_1(\beta)$ is impossible since branches (36) exist either for $\beta < 0$ or $\beta > 0$ only, depending on the sign of $z - 1$. Here we dis-

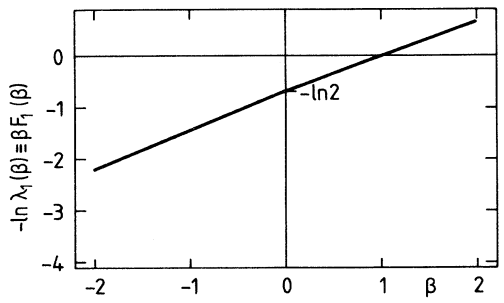


FIG. 5. Eigenvalue $\lambda_1(\beta)$ obtained by iterating the Frobenius-Perron equation with an initial function having singularities of type $(1 - 1/z)\beta$ at the two fixed points and at the origin. The plot is deduced from the $n = 12$th iteration. Parameters are the same as in Fig. 3.

cuss another mechanism which in special cases does lead to a double phase transition. Its explanation requires a deeper analysis of the iteration with eigenvalue $\lambda_1(\beta)$.

Let us consider the $n$th iterate of the starting function $\psi_0^{(\beta)}(x)$ having singularities $\sigma(\beta)$ at the origin and at the fixed points $[\sigma_i^{(0)} = \sigma(\beta), i = 1, \ldots, 4]$. This yields a function $\psi_n^{(\beta)}(x)$ converging toward a finite $\psi^{(\beta)}(x)$ if and only if the prefactor $R(\beta)$ is choosen to be the reciprocal of the largest eigenvalue $\lambda_1(\beta)$ in this function space, i.e.,

$$\lambda_1^n(\beta)\psi_n^{(\beta)}(x) = L_\beta^n \psi_0^{(\beta)}(x). \tag{40}$$

Since $\psi_n^{(\beta)}$ converges to a finite limiting function that is independent of $n$, but all other terms grow exponentially, the actual value of $\psi_n^{(\beta)}(x)$ becomes irrelevant for $n \to \infty$ and we can obtain $\lambda_1(\beta)$ as

$$\ln \lambda_1(\beta) = \lim_{n\to\infty} \frac{1}{n} \ln \left( \sum_{x=f^n(x_i)} \frac{\psi_0^{(\beta)}(x_i)}{| f^{n\prime}(x_i) |^\beta} \right). \tag{41}$$

The summation is taken here over all $n$th preimages $x_i$ of $x$ and the result is completely independent of the choice of $x$. Let us now underestimate $\lambda_1(\beta)$ by keeping in the sum one term only with $x_i = x^*$, where $x^*$ is just the preimage of $x$ closest to one of the fixed points

$$\ln \lambda_1(\beta) \geq \lim_{n\to\infty} \frac{1}{n} \ln \left( \frac{\psi_0^{(\beta)}(x^*)}{| f^{n\prime}(x^*) |^\beta} \right). \tag{42}$$

For sufficiently large $n$, the distance between $x^*$ and the fixed point scales with the slope at the fixed point, i.e.,

$$x^* + (1 + l_-) \sim c_4^{-n} \tag{43}$$

or

$$x^* - (1 + l_+) \sim c_1^{-n}, \tag{44}$$

depending on which fixed point is chosen. The slope of the $n$-fold iterated map is

$$| f^{n\prime}(x^*) | \approx c_1^n \quad \text{or} \quad c_4^n. \tag{45}$$

Since the starting fuction near the fixed point is

$$\psi_0^{(\beta)}(x^*) \approx A_4^{(0)}(x^* + 1 + l_-)^{-\sigma(\beta)} \tag{46}$$

or

$$\psi_0^{(\beta)}(x^*) \approx A_1^{(0)}(x^* - 1 - l_+)^{-\sigma(\beta)}, \tag{47}$$

we find

$$\frac{\psi_0^{(\beta)}(x^*)}{| f^{n\prime}(x^*) |^\beta} \sim c_{1(4)}^{n(\sigma(\beta)-\beta)}. \tag{48}$$

From (31) and (48)

$$-\ln \lambda_1(\beta) \leq +\frac{\beta}{z} \ln c_{1(4)} \tag{49}$$

follows, providing an upper bound for $\beta F_1(\beta)$ (see Fig. 6). Note that this upper bound is valid for any values of $\beta$.

There are two exceptional cases where the upper bounds force the free energy to behave anomalously, which can lead to an additional phase transition different from those discussed in Sec. IV. In fact, the new transition is connected with branch $F_1(\beta)$ and, in view of (39), generates a phase transition in the entropies, provided a natural measure exists.[17] The special cases in question are when one of the main fixed points is either superunstable ($c_{1(4)} = \infty$) or is marginally unstable ($c_{4(1)} = 1$).

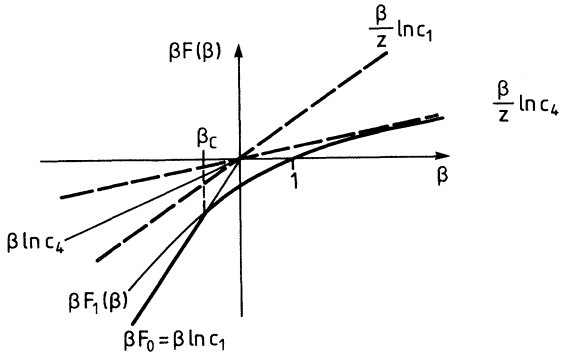


FIG. 6. Schematic plot of the free energy (heavy line) for $z > 1$, the branches (36), and the upper bounds provided by Eq.(49) (dashed lines).

To be more specific, let us consider first the case of extreme instability (say, $c_1 = \infty$). Due to the anomalous scaling at the right fixed point[17] the branch $-\ln \lambda_1(\beta)$ is then chopped off at $\beta = 0$ : $\beta F_1(\beta)\,|_{\beta=0}$ is still finite since the topological entropy is $\ln 2$, but $F(\beta) = F_1(\beta) = \infty$ for all $\beta < 0$. The jump at $\beta_{c1} = 0$ can be interpreted as a (zeroth-order) phase transition. For maps with $z < 1$ the bound $\beta/z \ln c_4$ coming from the other fixed point lies for positive $\beta$ above the branch $\beta F_0 = \beta \ln c_4$ and the latter might, therefore, intersect the branch $\beta F_1(\beta)$. This results then in a second phase transition at some $\beta_{c2} > 0$ as depicted in Fig. 7(a). If the map possesses a natural measure, there is a phase transition also in the entropies at $q = 0$ and $K_q = \infty$ for all $q < 0$,[17] but the second transition at $\beta_{c2}$ is not reflected in the entropies; $K_q$ behaves smoothly at $q = \beta_{c2}$.

The marginally unstable case is connected with an intermittent chaotic dynamics[44] and was pointed out to be present in Lorenz-type flows too.[19] Without restriction of generality, let us choose the left fixed point to be marginal ($c_4 = 1$). It is known[8,11,21,29] that due to the nonexponential scaling of the cylinder containing the marginal fixed point, the free energy must identically vanish for $\beta \geq \beta_{c2} = 1$. The transition at $\beta = 1$ can be of infinite order.[29] For $z > 1$ Eq.(49) does not exclude the possibility of a crossing between branches $\beta F_1(\beta)$ and $\beta F_0 = \beta \ln c_1$ in the negative $\beta$ range. Thus if

$$c_4 = 1, \quad z > 1 \tag{50}$$

another phase transition might also occur at some $\beta_{1c} < 0$ as illustrated in Fig. 7(b).

As an example, we consider the map

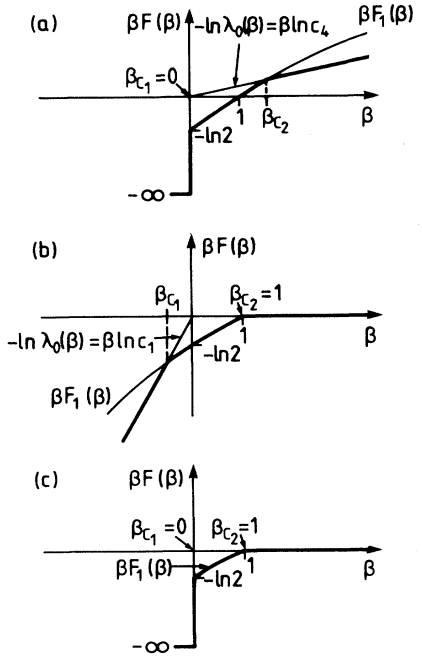


FIG. 7. Schematic diagram of double phase transitions in the free energy. (a) Superunstable case, $c_1 = \infty$, $z < 1$; (b) marginal case, $c_4 = 1$, $z > 1$ (strong intermittency); (c) mixed case, $c_1 = \infty$, $c_4 = 1$.

$$f(x) = \begin{cases} +(1+l_+)[(x-1)/l_+]^2, & 1 < x < 1+l_+ \\ -(1+l_-)(1-x)^z, & 0 < x < 1 \\ +(1+l_+)(x+1)^z, & -1 < x < 0 \\ d\cos[\omega(x+1)-1], & -1-l_- < x < -1, \end{cases} \tag{51}$$

where $d$ and $\omega$ are solutions to the irrational equations

$$d\omega \sin(\omega l_-) = 1, \quad d[\cos(\omega l_-) - 1] = -1 - l_-, \tag{52}$$

which ensure unit slope and completeness. For $l_+ = 0.9$ and $l_- = 1$ one obtains $d = 0.922\ldots, \omega = 3.537\ldots$. By solving Eq.(13) iteratively with a constant initial function we found the free energy quite accurately in the range $\beta < 1$ after $n = 15$ steps. The convergence is much worse in the intermittent phase $\beta > 1$ where only a slow decay towards the exact result can be observed (Fig. 8).

Finally, let us discuss the existence of a natural measure for cases with a double phase transition. While there is no general reason for excluding its existence from the superunstable case, it can never exist in cases caused by intermittency. To see this, let us consider the Frobenius-Perron equation (11). Writing it for $x' \to -1 - l_-$ we find

$$\varrho(x)\,|_{x\to -1-l_-} = \frac{\varrho[(x+1+l_-)/c_4 - 1 - l_-]}{c_4} + \frac{\varrho[(x+1+l_-)/c_3]}{c_3}. \tag{53}$$

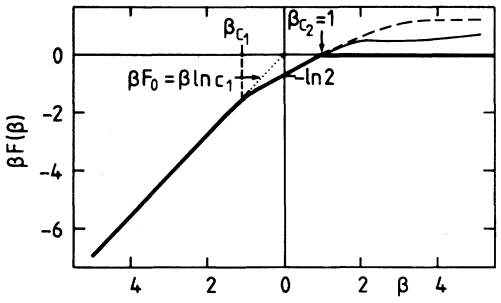


FIG. 8. Free energy (heavy line) of map (51). Dashed and thin lines stand for the iterates $n = 12$ and 15, respectively, of a constant function. For $\beta < 1$ they practically coincide, but the convergence is much slower for $\beta > 1$. The dotted line denotes the branch $\beta F_0 = \beta \ln c_1$. For the phase transition in the negative temperature range $\beta_{1c} = -1.057 \pm 0.001$ was found.

Since $c_4 = 1$ this shows that $\varrho(x)$ must diverge at the left fixed point unless it vanishes for $x \to 0$. Equation (27), taken at $\beta = 1$, however, tells us that the density $\varrho$ diverges for $z > 1$. Thus the first possibility remains. A more detailed analysis[43,47,48] also shows that for Taylor expandable maps around the fixed point, $\varrho$ diverges as $(x+1+l_-)^{-(2-1/z)}$, i.e., the density is not normalizable.

Therefore we conclude that condition (50) excludes the possibility of a *weak* intermittency[48] characterized by the existence of a well-defined invariant density. Rather it involves *strong* intermittency having a non-normalizable invariant density $\varrho(x)$ describing the fact that typical trajectories spend the majority of their lifetime around the marginal fixed point. In such cases generalized entropies cannot be defined. [We note in passing that in weak intermittent cases which can be realized for $z < 1$ generalized entropies exist and show a phase transition: $K_q\,|_{q=\beta} = 0$ for $\beta \geq \beta_{c2} = 1$ (Refs. 8 and 11), corresponding to the transition in the free energy at $\beta = 1$. Then, however, no second transition can occur since (50) does not hold.]

As a last comment we point out the possibility of a double phase transition in $F_1$ or in the entropies. This might take place when the aforementioned special conditions are simultaneously fulfilled, i.e., when one of the fixed points is superunstable and the other is marginal: $c_1 = \infty$ and $c_4 = 1$. Then from upper bounds (49) follows that $F_1 = F = \infty$ for $\beta < 0$ and $F_1 = F = 0$ for $\beta > 1$. Consequently, a nontrivial free energy exists in the range $0 \leq \beta < 1$ only [Fig.7(c)]. In this case the branch $\beta F_0$ does not play any role and exponent $z$ can be chosen arbitrarily. For $z < 1$, a natural measure might exist which is connected then with a double phase transition in the entropies: $K_q = \infty$ for $q < 0$, $K_q$ is finite and different from zero in the range $0 \leq q \leq 1$, and $K_q = 0$ for $q > 1$. This is, however, in a sense, a codimension-two situation to which two parameters are to be properly chosen, which illustrates the rule that phase transitions in entropies are less typical. In other words, the entropy spectrum is invariant under a broader class of transformations than the free energy.

## VI. THERMODYNAMICS OF THE PIECEWISE LINEAR CASE

As mentioned in Sec. IV, the singularity analysis does not work for $z = 1$ because $\sigma(\beta) \equiv 0$ in this case. The first-order phase transition and the condensed phase do not appear then. For $z = 1$ the branches of map (21) are linear functions of $x$. This special feature allows us to determine the free energy $F(\beta)$ exactly and to construct a physical system, namely an Ising chain, whose free energy per spin is just $F(\beta)$ at temperature $1/\beta$. This remarkable analogy helps us to illustrate the meaning of phase transitions and ground-state energies in the thermodynamic formalism.

Let us consider the iterative solution of the GFPO (15) starting from a constant function $\psi_0^{(\beta)} \equiv 1$ for map (21) with $z = 1$. The first iteration produces a piecewise constant function:

$$\psi_1^{(\beta)}(x) = \begin{cases} R(\beta)(a_1^{-\beta} + a_2^{-\beta}) = c_1^+, & x > 0 \\ R(\beta)(a_3^{-\beta} + a_4^{-\beta}) = c_1^-, & x < 0 \end{cases} \tag{54}$$

where $a_1 = (1+l_+)/l_+$, $a_2 = (1+l_+)$, $a_3 = (1+l_-)$, and $a_4 = (1 + l_-)/l_-$. In further iteration steps the iterated function $\psi_n^{(\beta)}(x)$ remains piecewise constant, of type (54), and the GFPO reduces to a matrix

$$L_\beta = \begin{pmatrix} a_1^{-\beta} & a_2^{-\beta} \\ a_3^{-\beta} & a_4^{-\beta} \end{pmatrix}, \tag{55}$$

acting on the two-component vector $(c_n^+, c_n^-)$ where $\psi_n^{(\beta)} = c_n^\pm$ for $x \gtrless 0$ [see (16)]. The eigenvalues of matrix $L_\beta$ are

$$\lambda_\pm(\beta) = \tfrac{1}{2}(a_1^{-\beta} + a_4^{-\beta} \pm [(a_1^{-\beta} - a_4^{-\beta})^2 + 4a_2^{-\beta}a_3^{-\beta})]^{1/2}, \tag{56}$$

from which the free energy is obtained simply as

$$F(\beta) = -\frac{1}{\beta} \ln \lambda_+(\beta) \quad \text{for } 1/\beta \neq 0. \tag{57}$$

Note that for $\beta \to \infty$ the eigenvalues approach each other in modulus: both tend to zero since the $a$'s are larger than 1. Consequently, this can be interpreted as a second-order phase transition at temperature 0.

To construct spin system with identical thermodynamics we compare (2) with the partition function for an Ising chain ($S_i = \pm 1$)

$$\exp[-\beta F(\beta) n] = \sum_{\{S_i\}} \exp[-\beta E(S_1, ..., S_n) n], \tag{58}$$

where the summation is taken over all spin states of the chain, and $E$ and $F(\beta)$ are the internal energy of a microstate and the free energy of a macrostate per spin, respectively. Thus we conclude that the logarithm of the length scales of cylinders divided by $-n$ plays the role of the energy per spin for spin state $\{S_i\} \equiv \{\epsilon_i\}$ (Ref. 1)

$$-\frac{1}{n} \ln l(\epsilon_1, \ldots, \epsilon_n) = E(\epsilon_1, \ldots, \epsilon_n). \tag{59}$$

It is easy to check that the length scale $l(\epsilon_1, \ldots, \epsilon_n)$ is proportional to the product of the inverse slopes of the map. Consequently, we can write

$$l^\beta(\epsilon_1, \ldots, \epsilon_n) \sim \prod_{\epsilon_1, \ldots, \epsilon_{n-1}} \frac{1}{a^\beta(\epsilon_i, \epsilon_{i+1})}, \tag{60}$$

where the notation

$$\begin{aligned} a_1 &= a(+1,+1), \\ a_2 &= a(+1,-1), \\ a_3 &= a(-1,+1), \\ a_4 &= a(-1,-1) \end{aligned} \tag{61}$$

has been used. A comparison of relation (60) with the definition of transfer matrices[49] shows that matrix $L_\beta$ is essentially the transfer matrix for the Ising chain. We consider $\ln a(\epsilon_i, \epsilon_{i+1})$ as a function of two spin variables and make the ansatz

$$\ln a(\epsilon_i, \epsilon_{i+1}) = -(E_0 + h_1\epsilon_i + h_2\epsilon_{i+1} + J\epsilon_i\epsilon_{i+1}), \tag{62}$$

which is found to be fulfilled with

$$E_0 = -\frac{1}{4} \ln(a_1a_2a_3a_4) = \frac{1}{4} \ln \frac{l_-l_+}{(1+l_-)^2(1+l_+)^2}, \tag{63}$$

$$h_1 + h_2 \equiv h = -\frac{1}{2} \ln(a_1/a_4) = \frac{1}{2} \ln \frac{l_+(1+l_-)}{l_-(1+l_+)}, \tag{64}$$

$$J = -\frac{1}{4} \ln(a_1a_4/a_2a_3) = \frac{1}{4} \ln l_-l_+. \tag{65}$$

Using (59)–(64) we have

$$\sum_{\{\epsilon_i\}} l^\beta(\epsilon_1, ..., \epsilon_n) \sim \sum_{\{\epsilon_i\}} \exp\left[\beta\left(nE_0 + h\sum_{i=1}^{n} \epsilon_i + J\sum_{i=1}^{n-1} \epsilon_i\epsilon_{i+1}\right)\right], \tag{66}$$

where the surface effect of two spins $\epsilon_1$ and $\epsilon_n$ has been neglected, which is irrelevant in the thermodynamic limit $n \to \infty$. Equation (66) is the partition sum of an Ising chain with coupling $J$, in homogeneous magnetic field $h$. $nE_0$ is an energy constant which does not affect the thermodynamics. The condition $l_-, l_+ \leq 1$ [see (9)] guarantees

$$J < 0, \tag{67}$$

unless $l_+ = l_- = 1$. In the latter case $a_1 = \cdots = a_4 = 2$, which corresponds just to the Bernoulli shift and the thermodynamics is trivial $J = h = 0$. In what follows we assume $l_+, l_- < 1$.

For $\beta > 0$ the partition sum represents an antiferromagnetic Ising chain. In the negative $\beta$ range, after applying the transformation $\beta \to -\beta$, $J \to -J$, $h \to -h$, and $E_0 \to -E_0$, we can interpret the spin system as a ferromagnetic Ising chain. The behavior of sum (66) is governed by the two eigenvalues of the transfer matrix:

$$\sum_{\{\epsilon_i\}} l^\beta(\epsilon_1, \ldots, \epsilon_n) \sim C_+ \lambda_+^n(\beta) + C_- \lambda_-^n(\beta), \tag{68}$$

where $C_+$ and $C_-$ are two nonzero constants. Consequently, the free energy per spin in the Ising chain is the same as $F(\beta)$ of the piecewise linear map as given by (56) and (57).

In the low-temperature limit of the antiferromagnetic model ($\beta \to +\infty$), $(a_2 a_3)^{-\beta}$ dominates all the other terms under the square root in (56), therefore

$$F(\beta) \to \tfrac{1}{2} \ln (a_2 a_3), \tag{69}$$

which can be written as

$$F(\beta) \to -(E_0 - J). \tag{70}$$

It is worth noting that in this limit $-\ln \lambda_+(\beta)$ and $-\ln |\lambda_-(\beta)|$ approach each other [and $\beta F(\beta)$] in harmony with the fact that there is a phase transition for $\beta \to \infty$. The quantity $n(E_0 - J)$ is just the ground-state energy of the antiferromagnetic Ising model, since the sum $\sum S_i$ is zero in the antiferromagnetic phase as long as the field is not stronger than $2 | J |$ which is fulfilled in view of (64) and (65).

In the other low-temperature limit $\beta \to -\infty$ we recover one of the ground states of the ferromagnetic model ($\uparrow\uparrow\uparrow\uparrow$ or $\downarrow\downarrow\downarrow\downarrow$), depending on the sign of the magnetic field:

$$F(\beta) \to \begin{cases} \ln a_1 = -(E_0 + h + J) & \text{if } a_1 > a_4 \\ \ln a_4 = -(E_0 - h + J) & \text{if } a_1 < a_4. \end{cases} \tag{71}$$

For $\beta \to -\infty$ there is no phase transition since the ground state of the system is not degenerated due to the presence of the magnetic field. In the symmetric case, however, when $l_+ = l_-$ and $a_1 = a_4$, $a_2 = a_3$ (but $a_1 \neq a_2$ as long as $l_+ < 1$) the magnetic field vanishes and the thermodynamics is that of the standard Ising chain. Then the eigenvalues approach each other also for $\beta \to -\infty$ corresponding to the well-known second-order phase transition of the Ising chain at zero temperature.

From a dynamical point of view, one expects the free energy to be strongly related to a simple periodic orbit for $\beta \to \pm\infty$. In fact, for $\beta \to \infty$ a 2-cycle gives the dominating contribution, and the free energy is just the Lyapunov exponent of this periodic orbit [see (69)]. It depends on the choice of the initial point which element of the 2-cycle is visited first. This degeneracy is the dynamical origin of the phase transition in the antiferromagnetic case. Similarly, for $\beta \to -\infty$ a fixed point always dominates, and the free energy is its Lyapunov exponent (71). As long as the stabilities of the fixed points are different, no phase transition can be present. In the symmetric case the fixed points become equally unstable and represent two energetically degenerate ground states of the ferromagnetic Ising chain. In summary, we can say that hyperbolic cases might also exhibit phase transitions which are, however, completely different in nature from those induced by the anomalous scaling around fixed points of nonhyperbolic maps.

## VII. DISCUSSION

We have studied, in the spirit of the thermodynamic formalism, complete Lorenz-type maps (1) possessing a single-step memory. Our working tool was the generalized Frobenius-Perron operator, which provides a very convenient framework for the analysis. After reorganizing, the map was shown to be equivalent with another one without memory. A peculiarity of the latter is to have zero or infinite slopes (critical points) away from its discontinuity. Consequently, the natural measure or, more generally, the eigenfunctions of the GFPO exhibit singularities both in the critical points and in their first images, which are just fixed points in complete cases.

In the free energy $F$, which is connected with the largest eigenvalue $\lambda^*$ obtained in an iteration procedure with smooth initial function of the GFPO as $\beta F(\beta) = -\ln \lambda^*(\beta)$, different types of singular behaviors, called phase transitions, have been found.

*Type I. Short* range interactions (which can, in general, be of both ferromagnetic and antiferromagnetic type) in an associated Ising chain can result in a second-order phase transition at *zero* temperature ($\beta \to \pm\infty$). This type of interaction characterizes *hyperbolic* maps having no critical points ($z = 1$) and no marginally stable or extremely unstable periodic orbits. Since the transition is at zero temperature, the free energy (as well as the entropy spectrum) of the map does not show any singularities at any finite $\beta$.

*Type II.* Critical points of *nonhyperbolic* maps always introduce *long*-range interactions in the associated Ising chain.[9,12] Equivalently, the cylinder lengths containing the first images of the critical points exhibit anomalous but exponential scaling determined by the slopes there. In certain *finite* temperature range an anomalous cylinder might dominate the free energy. The point where it takes over the dominance corresponds to a phase transition. This class of transitions is typically of first order and appears for positive ($z < 1$) or negative ($z > 1$) temperatures only. Such transitions *never show up* by starting the iteration of the GFPO with an appropriate singular function, and have no influence on the generalized entropies.

*Type III.* The long-range interaction of the associated Ising chain can be either extremely strong or weak depending on whether the slope at certain fixed points is infinity or unity (superunstable or marginal case). The

cylinder lengths at the fixed points then no longer scale exponentially. The dominance of these boxes *cannot* be avoided by starting with singular functions in an iterative solution. The corresponding phase transition can be of extreme (zero of infinite) order and always appears in the spectrum of *entropies*,[27] provided a natural measure exists.

All three types of transitions can be present in usual single-humped maps. Double phase transitions at finite $\beta$ values, however, cannot be observed there. We pointed out the possibility of type-II–type-III double transitions in complete Lorenz-type maps. If superunstable and marginal fixed points coexist, a type-III–type-III transition shows up.

Finally, we briefly discuss special cases. The original inversion symmetry of the Lorenz model has not been used in the paper. This symmetry for map (1) means that $\phi_1(x) = -\phi_4(-x)$ and $\phi_2(x) = -\phi_3(-x)$ (cf. Fig. 1), and $l_+ = l_-$. One can easily check[36] that the GFP equation for map (10) is then equivalent with one written for a reduced map

$$g(x) = \begin{cases} -\phi_2(x), & 0 < x < 1 \\ \phi_4(x), & -l_+ < x < 0 \end{cases} \tag{72}$$

shown in Fig. 9(a) for $z < 1$. Since now $c_1 = c_4$, double phase transitions are excluded. We mention in passing an interesting limiting case of maps (72) characterized by a jump at $x = 0$ which attracted recent interest.[37,50]

Another special class of Lorenz-type maps is provided if the memory is not present, which means $l_+ = l_- = 1$ and $\phi_1 = \phi_2, \phi_3 = \phi_4$.[39] Such a map is illustrated in Fig. 9(b) for $z > 1$. In the absence of further symmetry the slopes at the two fixed points are different $c_1 \neq c_4$. Consequently, all the phenomena found in map (10) can already be present in this simpler case. An even richer thermodynamics is expected if the orders of extrema are not all equal in this map, or in (10), but its study is already beyond the scope of this paper.

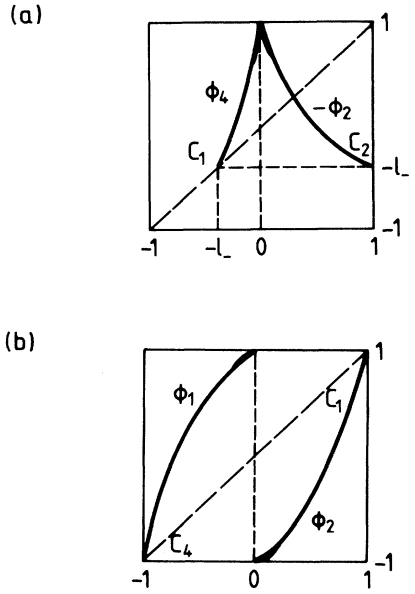


FIG. 9. Special cases of map (1). (a) Equivalent reduced map in presence of inversion symmetry ($z < 1$). (b) Lorenz-type map without memory ($z > 1$).

## ACKNOWLEDGMENTS

Illuminating discussions with Z.Kaufmann are acknowleged. Two of us (T.T. and G.V.) would like to thank Professor G. Eilenberger for the kind hospitality at the Institut für Festkörperforschung of the Forschungszentrum Jülich GmbH. This work was partially supported by the Hungarian Academy of Sciences (Grant No. OTKA 819). G.V. thanks the financial support of the Foundation for Hungarian Science.

*On leave of absence from Institute for Theoretical Physics, Eötvös University, Budapest, Hungary.
†On leave of absence from Institute for Solid State Physics, Eötvös University, Budapest, Hungary.

[1] Y. G. Sinai, Usp. Mat. Nauk. **27**, 21 (1972) [Russ. Math. Surveys **166**, 21 (1972)]; R. Bowen, Lect. Notes Math. **470**, 1 (1975); D. Ruelle, *Thermodynamic Formalism* (Addison-Wesley, Reading, MA, 1978); D. H. Mayer, Lect. Notes Phys. **123**, 1 (1980); D. Ruelle, Phys. Rev. Lett. **56**, 405 (1986); J. Stat. Phys. **56**, 405 (1986).
[2] M. J. Feigenbaum, M. H. Jensen and I. Procaccia, Phys. Rev. Lett. **56**, 1503 (1986).
[3] T. Bohr and D. Rand, Physica D **25**, 387 (1987).
[4] M. H. Jensen, L. P. Kadanoff, and I. Procaccia, Phys. Rev. A **36**, 1409 (1987); P. Collet, J. Lebowitz, and A. Porzio, J. Stat. Phys. **47**, 609 (1987); M. J. Feigenbaum, J. Stat. Phys. **46**, 919 (1987); **46**, 925 (1987); M. Kohmoto, Phys. Rev. A **37**, 1345 (1987); P. Alström, in *Time-Dependent Effects in Disordered Materials*, edited by R. Pynn and T. Riste (Plenum, New York, 1987); T. Bohr and T. Tél, in *Directions in Chaos*, edited by U. Bai-lin Hao (World Scientific, Singapore, 1988), Vol. II; A. Arneodo and M. Holschneider, J. Stat. Phys. **50**, 995 (1988); A. O. Lopes, SIAM J. Math. Anal. **20**, 1243 (1989).
[5] M. J. Feigenbaum, in *Nonlinear Evolution and Chaotic Phenomena*, edited by G. Gallavotti and P. F. Zweifel (Plenum, New York, 1988); J. Stat. Phys. **52**, 527 (1988).
[6] T. Tél, Z. Naturforsch. **43A**, 1154 (1988); R. Badii, Riv. Nuovo Cimento **12**, 1 (1989); A. B. Chhabra, R. V. Jensen, and K. R. Sreenivasan, Phys. Rev. A **40**, 4593 (1989).
[7] P. Cvitanović, in *Group Theoretical Methods in Physics*, edited by R. Gilmore (World Scientific, Singapore, 1987).
[8] P. Szépfalusy and T. Tél, Phys. Rev. A **35**, 477 (1987).
[9] D. Katzen and I. Procaccia, Phys. Rev. Lett. **58**, 169 (1987).
[10] R. Badii and A. Politi, Phys. Rev. A **35**, 1288 (1987); Phys.

Scr. **35**, 243 (1987).
[11]P. Szépfalusy, T. Tél, A. Csordás, and Z. Kovács, Phys. Rev. A **36,** 3525 (1987).
[12]M.H.Jensen and T.Bohr, Phys. Rev. A **36,** 4904 (1987).
[13]T. Horita *et al.*, Prog. Theor. Phys. **80**, 793 (1988); H. Hata *et al.*, *ibid.* **80**, 809 (1988); T. Yoshida *et al.*, *ibid.* **82**, 879 (1989).
[14]E. Ott, C. Grebogi, and J. A. Yorke, Phys. Lett. A **135**, 343 (1989).
[15]P. Grassberger, R. Badii, and A. Politi, J. Stat. Phys. **51**, 135 (1988).
[16]P. Szépfalusy, Phys. Scr. **T25**, 226 (1989).
[17]A. Csordás and P. Szépfalusy, Phys. Rev. A **39,** 4767 (1989).
[18]A. Csordás and P. Szépfalusy, Phys. Rev. A **40,** 2221 (1989).
[19]Z. Kaufmann and P. Szépfalusy, Phys. Rev. A **40,** 2615 (1989).
[20]J. Bene, P. Szépfalusy, and A. Fülöp, Phys. Rev. A **40,** 6719 (1989).
[21]X.-J.Wang, Phys. Rev. A **39,** 3214 (1989); **40**, 6647 (1989); A. O. Lopes (unpublished).
[22]P. Kluiving, H. W. Capel, and R. A. Pasmanter, Physica A **164**, 593 (1990).
[23]P. Szépfalusy and T. Tél, Phys. Rev. A **34,** 2520 (1986); T. Tél, Phys. Lett. A **119**, 65 (1986); Phys. Rev. A **36,** 1502 (1987).
[24]T. Tél, Phys. Rev. A **36,** 2507 (1987).
[25]P. Szépfalusy and U. Behn, Z. Phys. B **65**, 337 (1987).
[26]H. Fujisaka and M. Inoue, Prog. Theor. Phys. **78**, 268 (1987).
[27]A. Csordás and P. Szépfalusy, Phys. Rev. A **38,** 2582 (1988).
[28]I. Procaccia and R. Zeitak, Phys. Rev. Lett. **50**, 2511 (1988); S. Vaienti, J. Phys. A **21**, 2023 (1988); **21**, 2313 (1988); J. Bene, Phys. Rev. A **39,** 2090 (1989); Z. Kovács, J. Phys. A **22**, 5161 (1989).
[29]M. J. Feigenbaum, I. Procaccia, and T. Tél, Phys. Rev. A **39**, 5359 (1989).
[30]H. Mori *et al.*, Prog. Theor. Phys. **81**, 60 (1989).
[31]Z. Kovács and T. Tél, Phys. Rev. A **40,** 4641 (1989).
[32]E. N. Lorenz, J. Atmos. Sci. **20**, 130 (1963); **20**, 167 (1963).
[33]T. Rikitake, Proc. Cambridge Philos. Soc. **54**, 89 (1958).
[34]O. E. Rössler, Z.Naturforsch. **31A**, 1664 (1976).
[35]J. A. Yorke and E. D. Yorke, J. Stat. Phys. **21**, 263 (1979).
[36]P. Szépfalusy and T. Tél, Physica D **16**, 252 (1985).
[37]Z. Kaufmann, P. Szépfalusy, and T. Tél, Acta Phys. Hung. **62**, 321 (1987).
[38]J. Guckenheimer, in *The Hopf Bifurcation and its Applications*, edited by Marsden and McCracken (Springer, New York, 1976).
[39]A. Arneodo, P. Coullet, and C. Tresser, Phys. Lett. **81A**, 197 (1981); J. M. Gambaudo *et al.*, Phys. Rev. Lett. **57**, 925 (1986); I. Procaccia, S. Thomae, and C. Tresser, Phys. Rev. A **35,** 1884 (1987).
[40]A. Rényi, *Probability Theory* (North-Holland, Amsterdam, 1970); P. Grassberger and I. Procaccia, Phys. Rev. A **28,** 2591 (1983).
[41]J. P. Eckmann and D. Ruelle, Rev. Mod. Phys. **67**, 617 (1985).
[42]J. P. Eckmann and I. Procaccia, Phys. Rev. A **34,** 659 (1986).
[43]G. Györgyi and P. Szépfalusy, J. Stat. Phys. **34**, 451 (1984).
[44]P. Manneville and Y. Pomeau, Commun. Math. Phys. **74**, 189 (1980).
[45]S. Grossmann and S. Thomae, Z. Naturforsch. **32A**, 1353 (1977).
[46]H. Kantz and P. Grassberger, Physica D **17**, 75 (1985).
[47]P. Szépfalusy and G. Györgyi, Phys. Rev. A **33,** 2852 (1986).
[48]S. Grossmann and H. Horner, Z. Phys. B **60**, 79 (1985).
[49]C. J. Thomson, in *Phase Transitions and Critical Phenomena*, edited by C. Domb and M. S. Green (Academic, New York, 1972).
[50]M. C. de S. Vieira, E. Lazo, and C. Tsallis, Phys. Rev. A **35,** 945 (1987); M. C. de Sousa Vieira and C. Tsallis, Europhys. Lett. **9**, 119 (1989); in *Instabilities and Nonequilibrium Structures II*, edited by E. Tirapegui and D. Villaroel (Kluwer Academic, Dordrecht, 1989); M. C. de Sousa Vieira and G. Gunaratne, Phys. Rev. A **41,** 1823 (1990).